J. Fluid Mech. (1979), *vol.* 90, *part* 2, *pp.* 315–325
Printed in Great Britain

Theory and experiments on the control of the stratification in almost-enclosed regions

By LARS RAHM AND GÖSTA WALIN

Department of Oceanography, University of Gothenburg,
Box 4038, 400 40 Gothenburg, Sweden

(Received 25 April 1977 and in revised form 5 June 1978)

A comparison is made between the theoretically predicted and the observed stratification in a container which is traversed by a prescribed flux of fluid. Two different geometries were used illustrating respectively a useful procedure for the control of a stratified laboratory system and a mechanism which is believed to be geophysically significant, e.g. for the control of the stratification in certain estuaries. The behaviour of the fluid system was in all cases characterized by an almost stagnant interior with a boundary layer at the non-horizontal wall of buoyancy-layer type. Agreement between theory and experiment was satisfactory within experimental errors, say 10 % of the overall temperature difference.

1. Introduction

A theoretical prediction of the stratification in an almost-enclosed region is compared with experiments on two cases with different geometries and boundary conditions. The theoretical description is based on a slight generalization of the theory for strongly stratified fluids given by Walin (1971, hereafter referred to as I) allowing a constant flux of fluid to pass through the container.

In the first case the container was cone-shaped, the conical surface being insulated and the base (facing upwards) held at a constant prescribed temperature. The conical shape was chosen to illustrate the effect of a cross-sectional area which increases upwards. It is believed that the mechanism illustrated by this case is of importance for estuaries with vertical variation of the cross-sectional area. The net flux through our laboratory container should thus be a very simple model of the cross-isohaline mass flux induced by the supply of sea water from outside the estuary. In the second case the container was a straight circular cylinder with a cylindrical wall of finite conductance. The theory and experiment for this case illustrate an exceedingly simple and efficient way to stratify a fluid in the laboratory. In fact the system described here is considerably simpler to handle in the laboratory than the system discussed in I. It is also believed that systems with essentially similar properties occur in many industrial applications.

2. Theory for arbitrary geometry

We shall study a strongly stratified fluid system, i.e. we expect

$$\left(\frac{\partial}{\partial x}, \frac{\partial}{\partial y}\right) T^I \ll \frac{\partial}{\partial z} T^I,$$

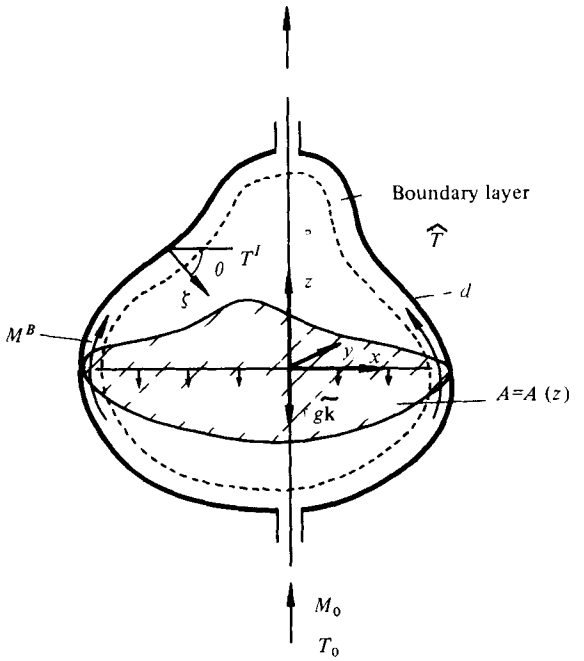

FIGURE 1. The general system described by (2.4). A container with wall thickness d is surrounded by a medium with controlled temperature $\hat{T}$. Fluid is pumped through the container at a rate M_0 and with an entrance temperature T_0. There is a transport M^B in the boundary layer which when added to the interior flow $w^I A(z)$ equals the inflow M_0. $A(z)$ represents the cross-sectional area of the container.

where T^I is the interior temperature distribution, z is the vertical co-ordinate and (x, y) the horizontal co-ordinates. As in I we formulate the theory within the Boussinesq approximation and we impose the following conditions:

$$\left(\frac{\kappa}{NL^2}, \frac{\nu}{NL^2}\right) \ll 1, \quad sL \ll \left(\frac{\nu}{NL^2}\right)^{-\frac{1}{2}}, \tag{2.1a, b}$$

the latter to be applied on every non-horizontal boundary. N is the buoyancy frequency, defined by $N^2 = g\alpha\Delta T/\rho_m L$, κ and ν are the diffusivities of heat and momentum, L is a typical length scale of the container, g is the gravitational acceleration, α is the coefficient of thermal expansion, ρ_m is the density of the fluid at some typical temperature, while s is a prescribed function of position on the boundary defined by the boundary condition on the temperature, viz.

$$\partial T/\partial\zeta = s(T - \hat{T}), \tag{2.2}$$

where ζ measures distance from the boundary. If the thermal conductivities of the wall and fluid are $\hat{k}$ and k and the wall thickness is d, s may be approximately identified with $\hat{k}/kd$ while $\hat{T}$ may be considered as a prescribed temperature outside the wall (see figure 1).

As discussed in I, (2.1a) restricts the diffusion of heat and momentum, giving rise to the boundary-layer character of the system, while (2.1b) restricts the thermal forcing, making the temperature difference across the boundary layer small compared with the temperature variations in the interior. The latter restriction is vital for the linearization of the boundary-layer equations, as was thoroughly discussed in I.

Under these conditions and assuming a steady state, we have the following equations describing the diffusive interior and the buoyancy layer at the non-horizontal wall to lowest order (see I):

$$T^I = T^I(z), \tag{2.3a}$$

$$w^I dT^I/dz = \kappa d^2T^I/dz^2, \tag{2.3b}$$

$$M^B = \kappa \frac{d}{dz} A - \oint \kappa s (T^I - \hat{T}) (\cos\theta dT^I/dz)^{-1} dl, \tag{2.3c}$$

$$M_0 = w^I A(z) + M^B, \tag{2.3d}$$

where w^I is the vertical velocity in the interior, $M^B(z)$ is the total transport carried by the boundary layer through a horizontal surface at height z, and $A(z)$ is the area inside the container of that surface. The symbol $\oint dl$ represents a line integral around the surface with area $A(z)$ and θ is the angle between the inward normal to the boundary and the horizontal plane ($-\frac{1}{2}\pi < \theta < \frac{1}{2}\pi$). (Note that dA/dz may be written as $-\oint \tan\theta\, dl$.)

The last equation (2.3d), expressing continuity of volume, represents a slight generalization compared with I in that we allow a net flux M_0 to pass through the container. Experimentally this means that we have holes at the top and bottom of the region allowing the fluid to be pumped through the container. Furthermore the inlet temperature of this flux has to be controlled.

Eliminating w^I and M^B from (2.3b, c, d), we obtain the following equation governing the interior temperature distribution:

$$\kappa A \frac{d^2T^I}{dz^2} + \left(\kappa \frac{dA}{dz} - M_0\right) \frac{dT^I}{dz} - \kappa \oint s \frac{T^I - \hat{T}}{\cos\theta} dl = 0. \tag{2.4}$$

The solution of (2.4) in general requires boundary conditions at the top and bottom of the region. [The boundary condition at the non-horizontal wall has already been taken care of in the derivation of (2.4).]

The problem discussed in I is obtained from (2.4) if M_0 is put to zero. We thus find that including a net flux traversing the region has added a first derivative dT^I/dz to the governing equation. This term changes the behaviour of the system in the limit of small interior diffusivity, i.e. when $sL \gg 1$.

(i) As discussed in I, when $M_0 \equiv 0$ and $sL \gg 1$ the main part of the region is controlled by the equation

$$\oint s \frac{T^I - \hat{T}}{\cos\theta} dl = 0. \tag{2.5}$$

This means that T^I is determined independently for each level. Consequently we obtain 'boundary layers' close to the top and bottom of the region where the first term in (2.4) is of importance and the solution adjusts to the boundary conditions.

(ii) When $M_0 \neq 0$ and $sL \gg 1$ we obtain in general

$$M_0 \frac{dT^I}{dz} + \kappa \oint s \frac{T^I - \hat{T}}{\cos\theta} dl = 0. \tag{2.6}$$

We thus find a first-order differential equation governing the degenerate interior. The presence of the first derivative in (2.6) makes it possible for solutions to this degenerate equation to satisfy one boundary condition, unlike solutions to (2.5). We thus expect

that one of the boundary layers present in the case $M_0 = 0$ should disappear. As may be shown by a straightforward boundary-layer analysis, (2.5) must satisfy the upstream boundary condition (as may be intuitively expected). Consequently the influence of this boundary condition penetrates throughout the interior while the downstream condition influences only a narrow region. For a further discussion of this case see § 4.

3. Insulated side walls: flow in a cone

We consider a container with an insulated non-horizontal wall, i.e. we put $s = 0$ in (2.4), which gives

$$\kappa A \frac{d^2T^I}{dz^2} + \kappa \frac{d}{dz} A \frac{dT^I}{dz} - M_0 \frac{dT^I}{dz} = 0, \tag{3.1}$$

or

$$\frac{d}{dz}\left(\kappa A \frac{dT^I}{dz}\right) = M_0 \frac{dT^I}{dz}. \tag{3.2}$$

Integrating twice and recalling that M_0 is constant, we obtain

$$T^I = C_1 \exp\left(\int_0^z \frac{M_0}{\kappa A}\, dz\right). \tag{3.3}$$

The boundary-layer transport M^B and the interior vertical velocity w^I are easily derived from (2.3) and become

$$M^B = \kappa(dA/dz) \tag{3.4}$$

and

$$w^I = (M_0 - M^B)/A. \tag{3.5}$$

The boundary-layer transport M^B and the interior vertical velocity w^I are thus independent of T^I.

The geometry of the experimental apparatus is illustrated in figure 2. The region under consideration was a half circular cone, i.e. it was enclosed by an upper horizontal surface, a conical surface and a vertical surface through the apex of the cone. The cone had a radius of 48·0 cm and the distance between the apex and the lid was 6·0 cm. The conical and the vertical surfaces were insulated ($s = 0$), while the horizontal surface was covered by a thin glass lid facing a constant-temperature bath with temperature T_1. The insulation of the conical surface was made of Styrofoam of minimum thickness 4·0 cm. The vertical wall was made of Plexiglas of thickness 2·0 cm, while the glass lid had a thickness of 0·4 cm. A constant net flux M_0 with inlet temperature T_0 was forced upwards through the container. In all our experiments T_0 was lower than T_1, which is obviously a necessary condition for a stable stratification to occur, i.e. for our theory to be applicable. Thus we have

$$A(z) = A_0 z^2/H^2, \tag{3.6a}$$

$$T^I = T_0 \quad \text{at} \quad z = 0, \tag{3.6b}$$

$$dT^I/dz = -s_1(T^I - T_1) \quad \text{at} \quad z = H, \tag{3.6c}$$

where A_0 is the area of the upper boundary and H is the total height of the region. s_1 is approximately determined by the thickness d of the glass lid and the heat conductivities of the glass and the fluid.

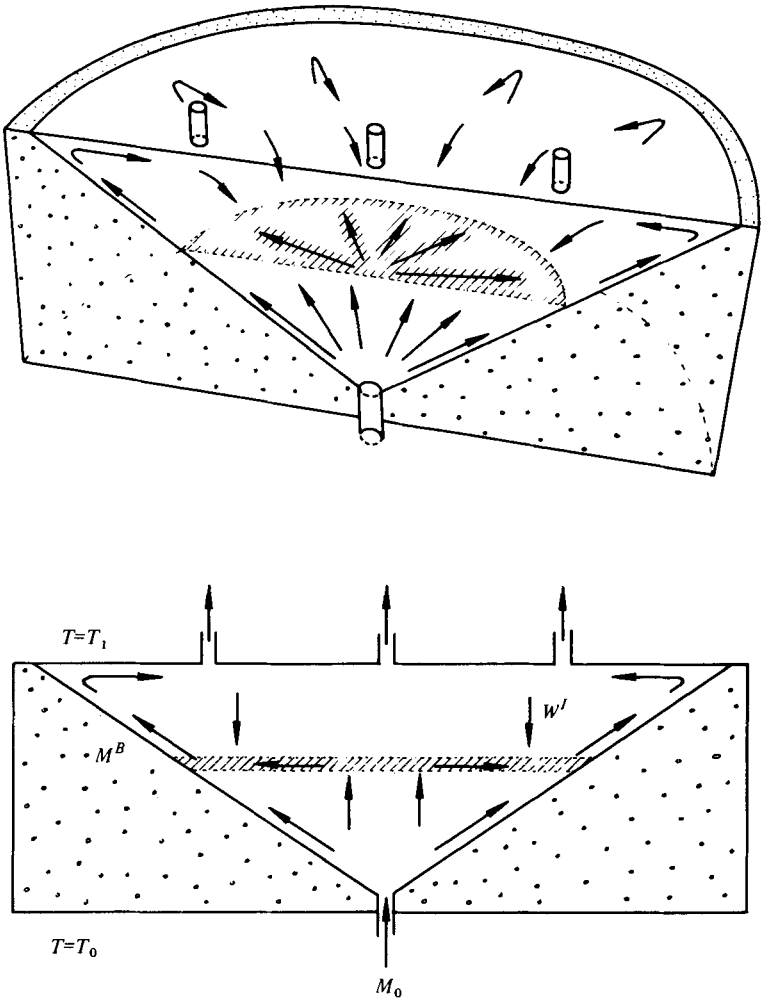

FIGURE 2. The experiment with a cone-shaped region. The sloping side is insulated and on the top there is a constant-temperature bath with temperature T_1. As illustrated, the interior temperature distribution will have an inflexion point which is shifted upwards when M_0 is increased. At this level the interior vertical velocity w^I is zero.

Applying (3.6) to our solution (3.3), we obtain

$$T^I - T_0 = \Delta T^* \exp(-H^*/z), \tag{3.7a}$$

where

$$\Delta T^* = (T_1 - T_0)(1 + H^*/s_1 H^2)^{-1} \exp(H^*/H), \tag{3.7b}$$

$$H^* = M_0 H^2/\kappa A_0. \tag{3.7c}$$

About ten experiments have been performed with different values of the external parameters M_0 and $T_1 - T_0$. In figure 3 we have collected the results from all our experiments in a diagram showing $(T^I - T_0)/\Delta T^*$ as a function of z/H^* (which in view of (3.7) should give us a single curve). Note that the value of z/H^* corresponding to the top of the region (i.e. $z = H$) varies between individual experiments.

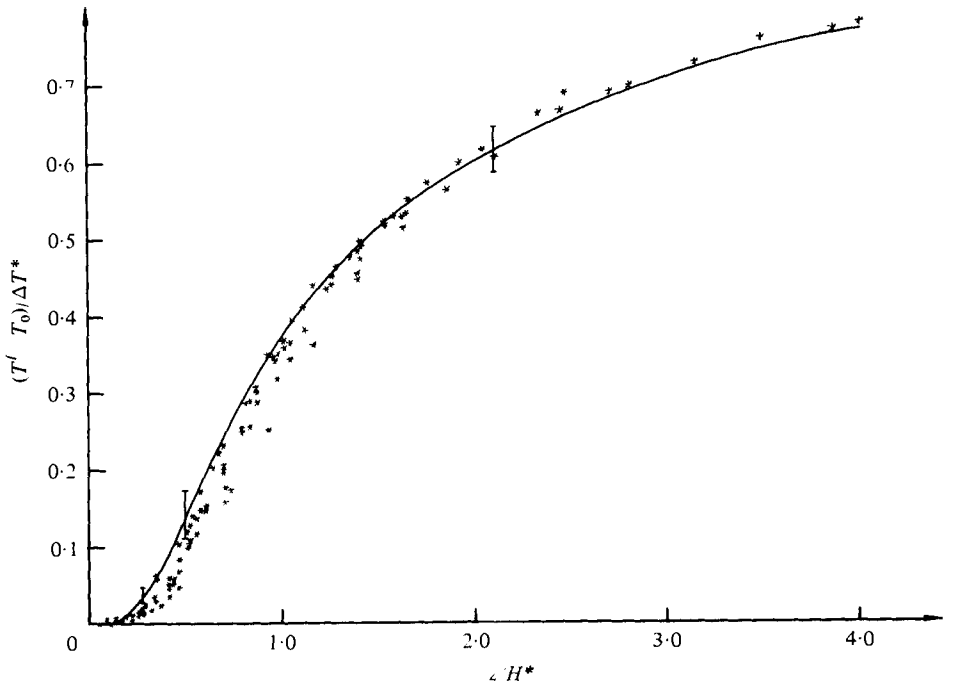

FIGURE 3. Temperature *vs.* depth in non-dimensional form from experiments and theory (solid curve) for a conical container. The scales ΔT^* and H^* are defined by (3.7*b*, *c*). Note that the level $z = H$ of the top boundary corresponds to different values of H/H^* for different experiments. The error bars on the predicted curve, illustrating the errors caused by uncertain conditions and external perturbations, have been calculated for $z = \frac{1}{2}H = 3$ cm with three different flow rates: $M_0 = 0{\cdot}2$, $0{\cdot}85$ and $1{\cdot}5\,\mathrm{cm}^3/\mathrm{s}$.

From (2.3*b*), (3.4) and (3.5) we reach the following conclusions.

(i) The sign of the vertical velocity w^I in the interior depends on whether or not the boundary-layer flux M^B exceeds the prescribed net flux M_0.

(ii) The sign of d^2T^I/dz^2 is determined by the sign of w^I.

(iii) At the level $z = \frac{1}{2}H^*$ we have $M^B = M_0$, i.e. w^I vanishes, and the temperature profile has an inflexion point (a 'thermocline'). This level will however fall outside the region if $H/H^* < \frac{1}{2}$.

In the experiment we could observe through the vertical part of the side wall the surface on which $M^B = M_0$ by injecting dye into the incoming water. This surface then stayed free of dye longer than any other part of the region. The circulation is illustrated in figure 2. It should be noted that the velocities in the interior are exceedingly small.

In the experiments M_0 was varied over the range $0{\cdot}2\,\mathrm{cm}^3/\mathrm{s} < M_0 < 1{\cdot}5\,\mathrm{cm}^3/\mathrm{s}$, which corresponds to $0{\cdot}5 < H/H^* < 4{\cdot}1$. By including time dependence in the analysis, it is easily shown that the time interval τ required for a steady state to be established is the so-called diffusion time, i.e. $\tau \sim H^2/\kappa$. In fact this remains true whenever the side walls are sufficiently well insulated in the sense that $sL \lesssim 1$. In our experiment we thus had $\tau \sim 7$ h.

4. The cylinder or an efficient way of stratifying a fluid

In this experiment we used a circular cylinder with its axis vertical. It was driven thermally by the vertical boundary (of constant thickness), outside which the temperature (T_1) was held constant. The whole container was made of Plexiglas. The radius of the cylinder was 7·0 cm and its height 33 cm. The thickness of the vertical wall was 0·5 cm. The bottom was insulated with a 5·0 cm thick sheet of Styrofoam. The lid had a thickness of 1 cm. As in the experiment with the cone a net upward flux M_0 was pumped through the container, the inflow being held at a constant temperature T_0 (see figure 4*a*). The lid was kept at approximately the temperature of the surrounding air ($\sim T_2$).

We thus have $$s = s_0, \quad \theta = 0, \quad A = A_0 = \pi R^2, \tag{4.1}$$

which when substituted in (2.4) give

$$\kappa A_0 \frac{d^2T^I}{dz^2} - M_0 \frac{dT^I}{dz} - 2\pi R s_0 \kappa (T^I - T_1) = 0. \tag{4.2}$$

Boundary conditions on (4.2) are obtained from continuity of heat flux.

At the lower boundary, where inflow occurs, we have

$$A_0(\rho c w^I T^I - k dT^I/dz) = A_0 \hat{k} d^{-1}(T_0 - T^I) + \rho c M_0 T_0 \quad \text{at} \quad z = 0,$$

where the left-hand side represents the heat flux in the fluid at $z = 0$ and the right-hand side the flux in the boundary itself, ρc being the heat capacity/unit volume. We have thus assumed that the outside of the boundary is held at the same temperature as the inflowing water, a limitation which can easily be relaxed. Simplifying, we obtain

$$dT^I/dz = (s_L + M_0/\kappa A_0)(T^I - T_0), \tag{4.3a}$$

where $s_L = \hat{k}/kd$ represents the heat conductivity of the lower boundary. (In the experiment s_L was small.)

Considering now the upper boundary we have in a similar way

$$A_0(\rho c w^I T^I - k dT^I/dz) = A_0 \hat{k} d^{-1}(T^I - T_2) + \rho c M_0 T^I \quad \text{at} \quad z = H,$$

where T_2 is the temperature outside the upper boundary. Note that (for obvious physical reasons) T^I appears in the last term on the right-hand side instead of T_2. Simplifying, we obtain

$$dT^I/dz = s_T(T^I - T_2), \tag{4.3b}$$

where s_T represents the thermal properties of the upper boundary. We conclude that the boundary condition at the outflow boundary is identical to the case with $M_0 = 0$.

Equation (4.2) has the solution

$$T^I - T_1 = C_1 \exp \alpha_1 z + C_2 \exp \alpha_2 z, \tag{4.4a}$$

where

$$\alpha_1 = \frac{M_0}{2\kappa A_0}\left[1 - \left(1 + \frac{8\pi R s_0 \kappa^2 A_0}{M_0^2}\right)^{\frac{1}{2}}\right], \tag{4.4b}$$

$$\alpha_2 = \frac{M_0}{2\kappa A_0}\left[1 + \left(1 + \frac{8\pi R s_0 \kappa^2 A_0}{M_0^2}\right)^{\frac{1}{2}}\right], \tag{4.4c}$$

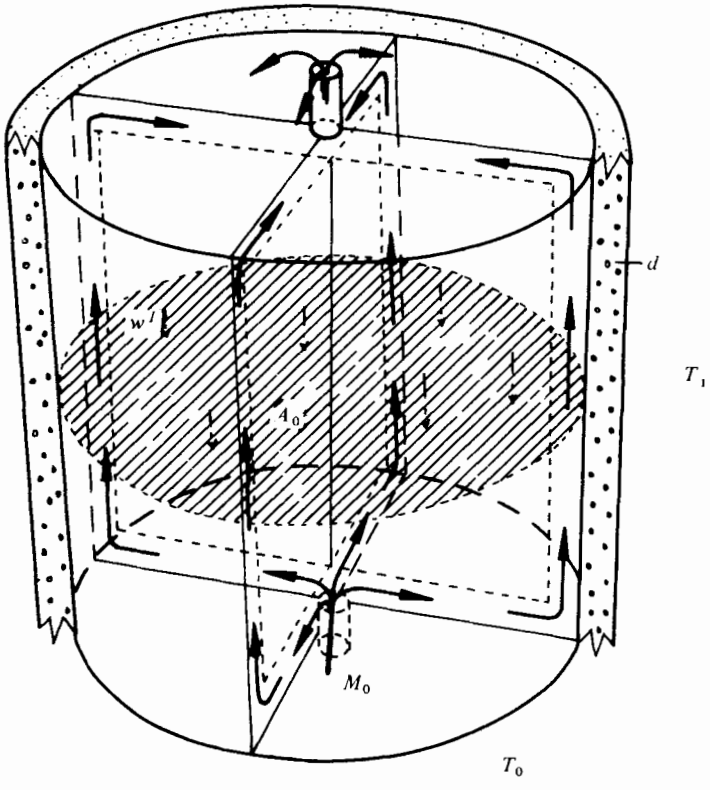

(*a*)

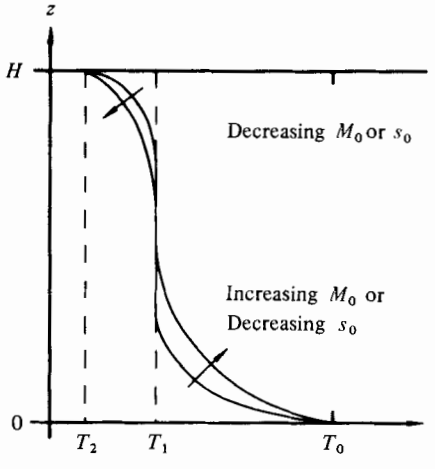

(*b*)

FIGURES 4 (*a*, *b*). For legend see opposite.

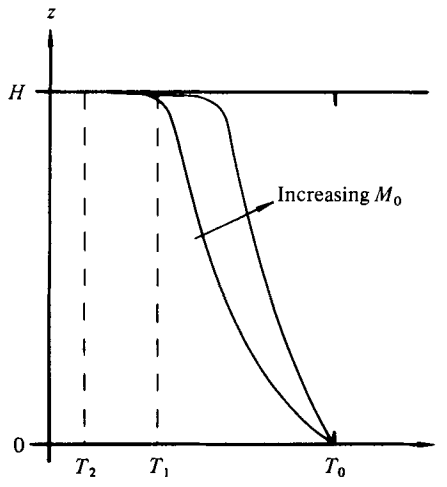

(*c*)

FIGURE 4. The cylinder and its dynamics. (*a*) shows that the vertical side wall is surrounded by a constant-temperature bath with temperature T_1. The inflow M_0 of temperature T_0 was pumped through the insulated bottom. A_0 is the cross-sectional area and w^I the interior vertical velocity. (*b*) illustrates the temperature distribution with a very small net flux M_0 and modest influence of vertical heat conduction. (*c*) illustrates the temperature distribution when M_0 is larger and vertical diffusion is unimportant except very close to the top. Our experiments were all in the range illustrated by (*c*).

and the constants C_1 and C_2 should be determined from the boundary conditions (4.3). The behaviour of (4.4) in different typical cases is illustrated in figures 4(*b*) and (*c*). As shown, the effect of increasing M_0 is to stretch out the lower exponential (the one which decays upwards) and squeeze the upper exponential. In the case illustrated in figure 4(*c*) the lower exponential dominates the solution except in a very thin layer at the top of the region. The upper boundary condition influences the solution only in this thin layer, as pointed out at the end of § 2.

Simplified description of experimentally important cases

In the limit $$M_0 H/\kappa A_0 \gg 1, \quad M_0 \sim RHs_0\kappa \tag{4.5}$$

(4.2) and (4.3*a*) degenerate to

$$M_0 dT^I/dz + 2\pi Rs_0\kappa(T^I - T_1) = 0, \tag{4.6a}$$

$$T^I - T_0 = 0 \quad \text{at} \quad z = 0. \tag{4.6b}$$

Equations (4.6) determine a solution which is valid everywhere except in a top layer of thickness $A_0\kappa/M_0$. The top boundary condition influences only this thin layer and should thus not be taken into account together with the degenerate equation (4.6*a*). Note that the form (4.6*b*) of the lower boundary condition results from (4.5) even if the lower boundary is completely insulated (i.e. if $s_L = 0$). The solution to (4.6) becomes

$$T^I - T_1 = (T_0 - T_1)\exp\alpha_1 z, \tag{4.7a}$$

where $$\alpha_1 = 2\pi Rs_0\kappa/M_0. \tag{4.7b}$$

From (2.3*c*) we have $$M^B = -\kappa s_0 2\pi R(T^I - T_1)(dT^I/dz)^{-1}. \tag{4.8}$$

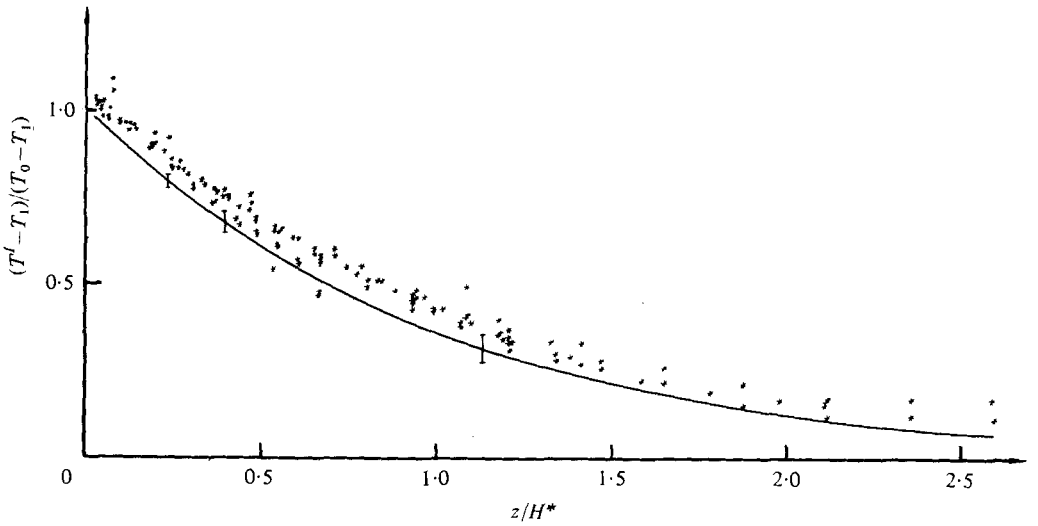

FIGURE 5. Temperature *vs.* depth in non-dimensional form from experiments and theory (solid curve) for a cylindrical container. T_0 is the temperature of the inflow, T^I is the interior temperature and T_1 is the temperature outside the side walls of the container. The theoretical prediction has been obtained from (4.7). The error bars have been calculated for $z = \frac{1}{2}H = 17{\cdot}5$ cm with three different flow rates: $M_0 = 0{\cdot}5$, $1{\cdot}5$ and $2{\cdot}5\,\mathrm{cm}^3/\mathrm{s}$.

We note that the boundary-layer transport associated with (4.7) is non-divergent (i.e. $dM^B/dz = 0$). In fact we have within the framework of (4.5)

$$M^B \gg w^I A \quad \text{or} \quad M^B \simeq M_0,$$

i.e. the vertical transport is dominated by the boundary-layer contribution.

The adjustment time τ is given by $\tau \sim H/\kappa s$, which is much less than the 'diffusion' time as discussed in I. In our experiment it is about 5 h.

In figure 5 all the measured data are presented together with the theoretical prediction given by (4.7). In the experiment M_0 was varied over the range

$$0{\cdot}5\,\mathrm{cm}^3/\mathrm{s} < M_0 < 2{\cdot}5\,\mathrm{cm}^3/\mathrm{s},$$

which corresponds to $0{\cdot}5 < -\alpha_1 H < 2{\cdot}5$, $80 < \alpha_2 H < 380$.

The thickness of the region influenced by the upper boundary condition ($\sim \alpha_2^{-1}$) was thus very small compared with H in the experiments.

5. Discussion of errors

The uncertainty in the theoretical prediction is due to uncertain external conditions and external perturbations. We estimate the variation in M_0 to be at most 10 %. The external temperatures T_0 and T_1 were estimated to vary within 1 % of the prescribed temperature difference.

We neglect variations in wall thickness in both experiments. In the case of the cone, there was some mixing near the apex induced by the inflow. This forced us to use the measured temperature T_h at the level $z = h$ ($= 0{\cdot}5$ cm) just above the apex as our boundary condition. The mixing was visualized by injecting dye into the incoming water and observing it through the thick vertical Plexiglas wall.

The errors are shown in figures 3 and 5 by error bars in the predicted curve. The errors have been calculated for $z = \frac{1}{2}H$ with three different flow rates in both experiments. There is a good agreement between theory and experiment in both cases. But, especially in the experiment with the cylinder, there is a systematic shift of the observations towards lower temperatures compared with the predicted values.

6. Main conclusions

The theory for strongly stratified fluids and the associated boundary layers has been verified through comparison with two widely different but simple experimental set-ups.

The first case, involving flow in a cone with insulated side walls, has some resemblance to the flow in an estuary. The importance of the topography for the vertical flux through the system and for the formation of a thermocline-like temperature structure is demonstrated.

The second case illustrates a very simple method of producing and maintaining a stratified system in the laboratory or elsewhere. It is believed that the principle demonstrated could be useful in industrial applications when accurate control of the temperature field is required.

We appreciate the assistance given by the staff at the Institute, especially Kristina Hansson, Agneta Hilding and Ulf Jonasson.

REFERENCE

WALIN, G. 1971 Contained non-homogeneous flow under gravity or how to stratify a fluid in the laboratory. *J. Fluid Mech.* **48**, 647.